VETERINARIA ITALIANA
RIVISTA DI SANITÀ PUBBLICA VETERINARIA

Paper

NMR-based-Metabolomics Evaluation in Dogs Infected with Canine Parvovirus: A New Approach for Biomarker/s

Abdullah Basoglu[1*], Rumeyhisa Ozlem Bicici[2], Francesca Di Cesare[3], Nuri Baspinar[2], Leonardo Tenori[4], Merve Ider[2], Erdem Gulersoy[5]

[1]*Department of Internal Medicine, Faculty of Veterinary Medicine, Near East University, Nicosia, Cyprus - TR*
[2]*Department of Internal Medicine, Faculty of Veterinary Medicine, Selcuk University, Konya Turkey - TR*
[3]*Magnetic Resonance Center (CERM) and Department of Chemistry "Ugo Schiff", University of Florence, Florence, Italy - IT*
[4]*Consorzio Interuniversitario Risonanze Magnetiche MetalloProteine (CIRMMP), Florence, Italy - IT*
[5]*Department of Internal Medicine, Faculty of Veterinary Medicine, Harran University, Şanlıurfa, Turkey - TR*

[*]*Corresponding author at: Department of Internal Medicine, Faculty of Veterinary Medicine, Near East University, Nicosia, Cyprus - TR*
E-mail: abdullah.basoglu@neu.edu.tr

Veterinaria Italiana, Vol. 61 No. 1 (2025) DOI: 10.12834/VetIt.3578.29616.2

Abstract

Despite aggressive treatment, canine parvovirus (CPV) enteritis remains a major cause of morbidity and mortality in puppies. Identifying reliable biomarkers of CPV enteritis is important for determining severity, length of hospital stay, and predicting clinical outcomes. This the first study that aims to emphasize the relevance of the manuscript. Forty-three (43) CPV-infected dogs were diagnosed by a rapid antigen test kit and subsequent PCR, and 10 healthy dogs were enrolled. In this prospective study, metabolomics and cardiac troponin were measured by NMR and ELISA, respectively. The diseased dogs showed statistically significant lower levels of fructose, glucose, citrate, glycerate, glutamate, carnitine, glycine, formate, and higher levels of isoleucine, isovalerate, glycolate, and creatine compared with healthy dogs. The same analysis performed on lipid parameters showed statistically significant higher levels of cholesterol variants, fatty acyl variants, free cholesterol, glycerol backbone, and sphingomyelin and lower levels of phosphoglycerates and esterified cholesterol in the diseased groups. The changes in metabolomics could be attributed to energy deficit, fat mobilization, gluconeogenesis, tricarboxylic acid cycle deficiency, and multiple organ failure. Decreased citrate, and increased fatty acyl chain-CH_2CO and sphingomyelin levels will serve as the most useful biomarkers in the prognosis of dogs suffering from CPV infection.

Keywords

Biomarker, Canine Parvovirus, metabolomics, NMR

Introduction

Canine parvovirus is a leading cause of death in young dogs, and has been a prevalent pandemic among dogs for over 40 years (Mazzaferro et al., 2020; Mylonakis et al., 2016; Sullivan 2019). Canine parvoviral enteritis promotes sepsis and systemic inflammatory response syndrome and is still one of dogs' most common enteric diseases worldwide (Alves et al., 2020). The prognosis for survival often depends on the severity of clinical signs at the time that therapy is initiated. Clinical signs indicating hypovolemia poor perfusion and fever, along with low protein C level, increased cortisol level, low thyroxine level, lymphocyte count less than 1000/mL, and hypoalbuminemia have been associated with increased mortality. Overall, the prognosis for survival ranges from 60% to 90%, depending on the study, type of therapy, and individual patient response to treatment. Comorbidities such as canine coronavirus and gastrointestinal parasitism also increased patient morbidity and mortality. Without therapy, the prognosis is grim, with death occurring in more than 90% of patients (Ling et al., 2012). The clinician dealing with the CPV enteritis patient must decide which prognostic test to measure and what particular threshold value would constitute enough evidence to support a decision for euthanasia or continued treatment (Schoeman et al., 2013).

Metabolomics has been used to study many infectious diseases (Tounta et al., 2021; Bueno, 2022). The most common use of metabolomics is for clinical and diagnostic purposes, especially the analysis of disease-specific

How to cite: Basoglu et al. NMR-based-Metabolomics Evaluation in Dogs Infected with Canine Parvovirus: A New Approach for Biomarker/s. Veterinaria Italiana, Vol. 61 No. 1 (2025) DOI: 10.12834/VetIt.3578.29616.2

biomarkers with NMR-based or mass spectrometry-based metabolomics (Al-Sulaiti et al., 2023). In metabolomics, a wide range of metabolites and lipids present in a biological material can be identified, quantified, and characterized (Vignoli et al., 2023). Significant changes in various metabolic pathways show that sepsis caused by CPV fundamentally alters biochemical processes, indicating disruptions in catabolism and energy production. Metabolomic and lipidomic analysis of sepsis can provide insight into the metabolic response of the host to infection (Montague et al., 2022; Pacheco-Navarro and Rogers 2023). To the best of our knowledge, metabolomics studies conducted on dogs are limited. Recently, progress has been made in understanding the role of inflammation, inflammatory metabolites, and lipids in infectious diseases. While metabolic studies of viruses such as HIV, hepatitis B and C, and SARS-CoV-2 are frequently encountered in human medicine (Al-Sulaiti et al., 2023), it is rare for the same factors to be known for CPV. This work aimed to reveal new potential biomarkers representing the metabolic status of CPV-infected dogs by using NMR-based metabolome profile evaluation and providing possible clues into the pathogenic mechanisms of this pathology.

Material and Methods

Patient selection and groups

A total of forty-three (43) CPV-infected dogs (40 Anatolian shepherds and 3 Golden Retrievers, aged between 1.5 and 4 months) with a history of weakness, decreased appetite, diarrhea/hemorrhagic diarrhea, vomiting, and dehydration with or without fever were included in this study. The clinical signs were scored as per the method described earlier (Table I) (Nguyen et al., 2006). The dogs were found positive for CPV infection as confirmed initially by a rapid CPV antigen detection kit (Anigen CPV Ag, Immunochromatographic assay, sensitivity: 100%, specificity: 98.8%) followed by PCR targeting VP2 gene for confirmation of the disease (Eregowda et al., 2020). Conventional PCR is a recommended diagnostic technique for the detection of canine parvovirus, but not the rapid tests used in veterinary practice (Navarro et al. 2020). The dogs included in the study were not vaccinated against CPV infection. Supportive treatment consisting of broad-spectrum antibiotics (cefixime 30 mg/kg, IV + *metronidazole* 5-7 mg/kg IV), antiemetic (maropitant 0.1 mg/kg), anti-inflammatory drugs with intestinal effect (meloxicam 0.06 mg/kg SC) and antioxidant (acetylcysteine 20 mg/kg IV) was administered together with IV fluid (crystalloid + colloid + K supplement as needed). All 43 CPV-positive puppies enrolled in the study received treatment for CPV and 13 dogs of them died within 24-48 hours of hospitalization. The four groups considered in this study are; I) healthy control (HC, 10 Anatolian shepherd dogs, confirmed with clinical examination, and hematologic and biochemical analyses, aged between 1.5 and 4 months, belonged to Selcuk University Kangal Dog Research Unit); II) survivors at admission (S ad., 43 dogs); III) the same dogs, survivors at 72 hours (S 72 h, 30 dogs); IV), and died within 24-48 hours after admission, non-survivals (NS, 13 dogs). The study was conducted as per the guidelines of the Institutional Animal Ethics Committee and the experimental protocol was approved by the Committee on Use of Animals in Research of “Blinded for review”, Selcuk University Faculty of Veterinary Medicine (01.07.2021).

Clinical sign	Score
Temperature	
≤37.3	1
37.4–39.4	0
39.5–39.9	1
40.0–40.4	2
≥ 40.6	3
Mucus in stool	1
Watery stool	2
Blood in stool	3
Anorexia	1
Lethargy	1
Depression	1
Vomiting	1
Coughing	1

Table I. Clinical score used in canine parvovirus infected dogs.

How to cite: Basoglu et al. NMR-based-Metabolomics Evaluation in Dogs Infected with Canine Parvovirus: A New Approach for Biomarker/s. Veterinaria Italiana, Vol. 61 No. 1 (2025) DOI: 10.12834/VetIt.3578.29616.2

Blood Sampling

Blood samples were collected from all diseased dogs (43) at admission (S ad.) via vena cephalic into tubes with and without anticoagulant for different analyses. Another sample was taken from the living dogs (30) after 72 hours (30 survivors at hour 72, S 72 h), no blood sample was taken again from the dogs (13) that died within 24-48 hours (non-survivors, NS). Healthy dogs were sampled just once.

Cardiac troponin I (cTnI) values

Serum cTnI values were determined by ELISA (BT Lab E0106Ca Canine Troponin 1, Tn-1 ELISA KIT). This assay has been previously validated by demonstrating satisfactory precision values (Apple et al., 2008).

NMR Analysis

^{1}H-NMR spectroscopy sample preparation

The extraction of serum samples took place at “Blinded for review”, while the NMR measurements were conducted at the CERM/CIRMMP facility of the Instruct-ERIC Institute at the University of Florence in Italy.

To prepare the water-soluble serum samples, the dried samples were dissolved in 700 µL of $2H_2O$ (99.9 atom % D, Sigma Aldrich, St. Louis, Missouri, USA) and homogenized by whirling for 1 minute. Each sample was mixed with 70 µL of potassium phosphate buffer (pH 7.4; 1.5 M K_2HPO_4, 100% (v/v) $2H_2O$, 2 mM NaN_3, 5.8 mM deuterated TMSP). For the NMR analysis, 600 µL of each mixture was transferred into 5 mm NMR tubes (Bruker BioSpin s.r.l.).

As for the lipid serum dried extracts, they were dissolved in 700 µL of CDCl3 (99.8 atom % D, Sigma Aldrich, St. Louis, Missouri, USA) and vortexed for 1 minute to ensure homogeneity. 600 µL aliquots from each sample were placed into 5 mm NMR tubes (Bruker BioSpin s.r.l.) for analysis.

A 600 MHz spectrometer (Bruker BioSpin s.r.l; Rheinstetten, Germany), operating at a proton Larmor frequency of 600.13 MHz, was used to obtain one-dimensional (1D) ^{1}H-NMR spectra for each sample. The equipment was set up with a probe that included a z-axis gradient coil and a 5 mm PATXI ^{1}H-^{13}C-^{15}N. It also had an automated sample changer that kept the samples refrigerated, and an automatic tuning and matching unit (ATM). To ensure minimal temperature fluctuations (within ±0.1K at the sample), a BTO 2000 thermocouple was utilized. Before conducting measurements, the NMR tubes were kept inside the NMR probe head at 310K for a minimum of 5 minutes to allow the temperature to stabilize.

The Nuclear Overhauser Effect Spectroscopy pulse sequence (NOESY 1Dpresat; noesygppr1d.com; Bruker BioSpin) was employed to acquire one-dimensional ^{1}H-NMR spectra for both water- and lipid-soluble samples. The acquisition parameters included 98304 data points, a spectral width of 18028 Hz, an acquisition time of 2.73 s, a relaxation delay of 4 s, a mixing time of 0.01 s, and 64 scans. For more details on the configuration and settings of the 600 MHz spectrometer, readers are referred to previous publications (Basoglu et al., 2017, 2018, 2020; Vignoli et al., 2019).

^{1}H-NMR spectra processing

Before performing the Fourier transform, the free induction decays were multiplied by an exponential function that corresponded to a line-broadening factor of 0.3 Hz. The resulting spectra were automatically corrected for phase and baseline distortions and calibrated using TopSpin 3.2 software (Bruker BioSpin). The anomeric glucose doublet signal at 5.24 ppm was used as a reference for correcting serum aqueous extracts, while the chloroform singlet at 7.20 ppm served as a reference for the organic fractions.

Each water-soluble 1D ^{1}H-NMR spectrum was divided into 0.02 ppm chemical shift buckets in the range of 0.02-10.0 ppm. Their corresponding spectral areas were integrated using AMIX software (version 3.9.15, Bruker BioSpin). The regions between 4.62 and 4.75 ppm containing the residual H_2O signal were excluded to correctly perform the multivariate analysis. The dimension of the system was reduced to 483 bins.

Each lipid-soluble 1D ^{1}H-NMR spectrum was divided into 0.02 ppm chemical shifts buckets in the range of 0.02-6.5 ppm to correctly perform the multivariate analysis, for a total of 315 bins. Before pattern recognition, total integral normalization was applied to the spectra.

More information on analytical methods and spectral processing is detailed in our previous paper publications (Basoglu et al. 2017; Vignoli et al., 2019).

Metabolites and lipids assignment and quantification

How to cite: Basoglu et al. NMR-based-Metabolomics Evaluation in Dogs Infected with Canine Parvovirus: A New Approach for Biomarker/s. Veterinaria Italiana, Vol. 61 No. 1 (2025) DOI: 10.12834/VetIt.3578.29616.2

To identify and quantify metabolites in the ^{1}H NOESY spectra of serum water-soluble extracts a library of pure organic compounds' ^{1}H NMR spectra (BBIOREFCODE, Bruker BioSpin), and the available literature was used. A total of 28 metabolites were identified and quantified (relative intensities in arbitrary units) in all spectra.

For the NMR signals in the ^{1}H NOESY spectra of serum lipid-soluble extracts, assignments were based on literature. We assigned and quantified (relative intensities in arbitrary units) a total of 17 lipid features in all acquired spectra.

To determine the relative concentrations of metabolites and lipid features (expressed in arbitrary units), we used an in-house developed R script that integrated NMR peaks using standard line-shape analysis methods.

Statistical analyses

Multivariate analyses

Random Forest (RF) algorithm (Ali et al., 2012; Amaratunga et al., 2008; Chen et al., 2013)1 2 3 was employed for pairwise classification of the entire metabolic and lipidic profiles of the four groups (healthy control (HC), survivors at admission (S ad.), survivors at hour 72 (S 72 h), and non-survivors (NS) considered in this study. The following comparisons were performed: HC *vs* S ad., HC *vs* S 72 h, HC *vs* NS, S ad. *vs* NS, S 72 h *vs* NS, and S ad. *vs* S 72 h groups.

Univariate analyses

To assess differences between the four groups, we employed the non-parametric Wilcoxon Rank-Sum test (Neuhäuser, 2011; Wilcoxon, 1945). Additionally, we used the non-parametric Wilcoxon signed-rank test to examine pairwise differences between the S ad. and S 72 h groups. In this pilot study, we chose not to incorporate adjustments for multiple testing in our analysis to ensure the identification of potential biomarkers, albeit at the cost of an elevated risk of type I error.

Software

All calculations were performed in R (version 4.0.3). To generate RF classification models, the "random Forest" function, implemented in the R package Random Forest (Breiman 2001; Ali et al., 2012) was used to grow a decision forest composed of 1000 trees, using default parameters.

Results

Clinical picture and score

Signs of puppies were dehydration with temperature (2 dogs <37.3, 29 dogs 37.4-39.4, 3 dogs 39.4-39.9 and 6 dogs 40.0-40.4), diarrhea (11 dogs watery stool, 4 dogs mucus in stool, 25 dogs blood in stool), 38 dogs anorexia, 40 dogs lethargy, 40 dogs depression. Clinical signs comparison is in Table II.

The mean clinical score (CS) of NS dogs was significantly ($P < 0.05$) decreased than HC, S ad. and 72 h dogs. The mean CS of NS and S ad. dogs was significantly higher ($P < 0.05$) than HC and S 72 h dogs (Table I).

How to cite: Basoglu et al. NMR-based-Metabolomics Evaluation in Dogs Infected with Canine Parvovirus: A New Approach for Biomarker/s. Veterinaria Italiana, Vol. 61 No. 1 (2025) DOI: 10.12834/VetIt.3578.29616.2

Parameters	Healthy (n:10)	Survivors ad. (n:43)	Survivors 72 h (n:30)	Non-survivors (n:13)	P value
Temperature	**0**	**0**	**0**	**0**	
2 dogs <37.3	**(0-0)b**	**(0-2)b**	**(0-0)b**	**(0-1)a**	
29 dogs 37.4-39.4					**0.000**
3 dogs 39.4-39.9					
6 dogs 40.0-40.4					
Stool	**0**	**3**	**0**	**3**	
11 dogs watery stool	**(0-0)c**	**(2-3)a**	**(0-3)b**	**(3-3)a**	**0.000**
4 dogs mucus in stool					
25 dogs blood in stool					
Anorexia	0	1	0	1	
38 dogs	(0-0)	(1-1)	(0-0)	(1-1)	-
Depression	0	1	0	1	
40 dogs	(0-0)	(1-1)	(0-0)	(1-1)	-
Letargy	0	1	0	1	
40 dogs	(0-0)	(1-1)	(0-0)	(1-1)	-
Vomiting	0	1	0	1	
0	(0-0)	(1-1)	(0-0)	(1-1)	-
Coughing	0	0	0	0	
0	(0-0)	(0-0)	(0-0)	(0-0)	1.000

Table II. Clinical signs comparing.

Cardiac troponin level

In the present study, cardiac troponin levels were not different between groups.

NMR evaluation

Water-soluble extracts

RF classification algorithm was applied to investigate whether the different four groups (HC, S ad., S 72 h, NS) could be discriminated from the entire metabolic profiles. The results of the RF classification for each comparison (HC *vs* S ad.; HC *vs* S 72 h; HC *vs* NS; S ad. v*s* NS; S 72 h *vs* NS groups; S ad. *vs* S 72 h) were given in Figure 1, respectively. Overall, we obtained extremely robust classification models to discriminate between the different groups: HC *vs* S ad. (Accuracy = 85%), HC *vs* S 72 h (Accuracy = 80%), HC *vs* NS (Accuracy = 91.3%), S ad. *vs* NS (Accuracy = 62.8%), S 72 h *vs* NS (Accuracy = 76.7%), and S ad. *vs* S 72 h (Accuracy = 76.7%).

How to cite: Basoglu et al. NMR-based-Metabolomics Evaluation in Dogs Infected with Canine Parvovirus: A New Approach for Biomarker/s. Veterinaria Italiana, Vol. 61 No. 1 (2025) DOI: 10.12834/VetIt.3578.29616.2

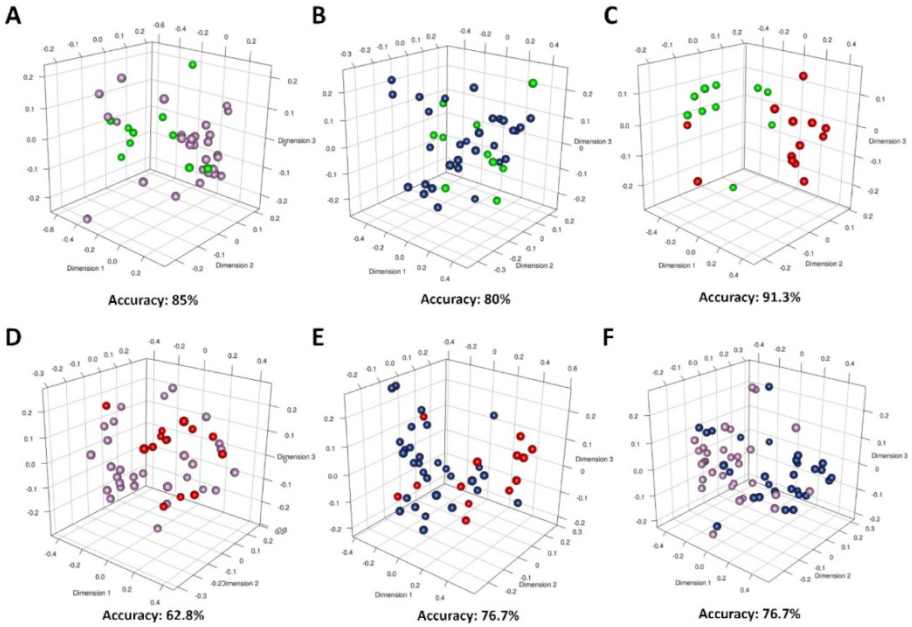

Figure 1. Random Forest (RF) model score plots. Each dot represents a single water-soluble serum metabolic profile colored by the different groups: A) HC (green dots) vs S ad. (violet dots) groups; B) HC (green dots) vs S 72 h (blue dots) groups; C) HC (green dots) vs NS (red dots) groups; D) S ad. (violet dots) vs NS (red dots) groups; E) S 72 h (blue dots) vs NS (red dots) groups; F) S ad. (violet dots) vs S 72 h (blue dots) groups. For each RF model performed the discrimination accuracy was also reported.

How to cite: Basoglu et al. NMR-based-Metabolomics Evaluation in Dogs Infected with Canine Parvovirus: A New Approach for Biomarker/s. Veterinaria Italiana, Vol. 61 No. 1 (2025) DOI: 10.12834/VetIt.3578.29616.2

	Healthy (n:10)	Survivors ad. (n:43)	Survivors 72 h (n:30)	Non-survivors (n:13)
Metabolites (relative intensities in arbitrary units)				
Glucose	7.06±1.21	5.36±1.98	5.85±2.14	5.33±2.52
Mannose	0.52±0.09	0.49±0.12	0.49±0.15	0.56±0.19
Tyrosine	3.54±0.43	4.35±0.71	3.95±0.71	3.99±0.9
Phenylalanine	0.37±0.05	0.46±0.1	0.46±0.17	0.47±0.13
Cholate	0.03±0.03	0.06±0.09	0.1±0.11	0.05±0.08
2-hydroxybutyrate	0.11±0.15	0.14±0.18	0.23±0.49	0.09±0.09
Isovalerate	0.22±0.12	0.31±0.16	0.32±0.17	0.43±0.16
Leucine	0.36±0.23	0.41±0.4	0.58±0.73	0.53±0.56
Isoleucine	0.33±0.38	0.87±0.41	0.85±0.55	0.58±0.49
Valine	0.1±0.05	0.15±0.15	0.14±0.16	0.17±0.25
3-hydroxybutyrate	0.23±0.2	0.29±0.4	0.32±0.38	0.26±0.54
Acetate	3.9±0.9	3.34±0.6	4.71±8.28	3.66±0.68
Glutamate	0.48±0.37	0.28±0.26	0.4±0.32	0.2±0.24
Pyroglutamate	0.07±0.03	0.06±0.02	0.06±0.03	0.06±0.03
Citrate	1.85±1.69	0.66±0.31	0.94±0.38	0.66±0.36
Creatine	1.15±0.66	1.53±0.84	1.18±0.85	2.36±1.57
Creatinine	0.97±0.5	0.64±0.28	0.76±0.57	0.94±0.67
Dimethylsulfone	0.32±0.29	0.59±0.47	0.49±0.42	0.57±0.56
Choline	1.17±0.29	1.17±0.54	1.25±0.58	1.42±0.57
Carnitine	0.38±0.11	0.25±0.16	0.3±0.17	0.26±0.13
Betaine + TMAO	22.78±15.73	21.43±13.52	18.69±9.02	19.08±10.94
Glycine	1.5±0.37	1.06±0.27	1.07±0.44	1.07±0.49
Glycerate	3±0.56	2.11±0.93	2.32±0.94	2.05±1.17
Glycolate	0.77±0.58	1.23±0.89	1±0.75	2.13±1.79
Fructose	3.53±0.5	3.05±0.52	3.03±0.64	2.80±0.81
Lactate	17.83±3.7	14.55±2.98	12.68±2.99	14.86±3.86
Formate	0.9±0.18	0.7±0.13	0.83±0.21	0.69±0.24
Alanine	0.3±0.14	0.34±0.14	0.33±0.24	0.52±0.52
Lipid parameters (relative intensities in arbitrary units)				
Total cholesterol C-18 H3	14.16±1.05	12.51 ±2.52	12.64±2.64	14.71±2.45
Fatty acyl chain $(CH_2)n$	286.35 ±12.25	276.14±25.8	268.48±31.42	274.07±25.47
Total_cholesterol	14.15±1.03	11.83±3.39	13.01±4.13	10.77±4.52
Fatty acyl chain -CH_2CH	20.79±1.67	19.19±3.86	19.35±2.93	20.69±2.79
Fatty acyl chain -CH_2CO	18.59±6.45	20.31±7.5	23.78±6.34	28.07±5.41
Fatty acyl chain $CHCH_2CH$	23.19±2.31	25.69±3.13	24.12±3.28	24.75±3.31
Phospolipids $n(CH_3)_3$	40.37±3.05	38.96±4.97	36.7±3.79	36.4±3.77
Free_cholesterol_X	2.09±0.6	2.49±0.49	2.92±0.46	2.78±0.36
Glycerol backbone C-1 H2 C-3 H2	0.38±0.17	0.53±0.24	0.64±0.2	0.77±0.25
Esterified cholesterol C-3 H	3.43±0.25	2.68±0.85	2.87±0.63	3.14±0.53
Phospoglicerides	5.29±0.41	5.28±0.47	5.02±0.53	4.89±0.5
Fatty acyl chain -HC=CH-	42.65±2.42	44.04±4.77	42.59±5.1	44.23±5.27
Sphingomyelin_CH=CH	0.68±0.11	0.77±0.23	0.92±0.15	0.89±0.14
Free cholesterol C-3 H	0.24±0.13	0.34±0.23	0.43±0.34	0.37±0.21
Total cholesterol C-26 H3 C-27 H3	10.72±0.9	9.48±2.03	9.78±2.21	11.16±1.84
Fatty acyl chain CH_3 $(CH_2)n$	2.26±0.32	2.28±0.42	2.32±0.38	2.22±0.21
Esterified cholesterol C-19 H3	1.35±0.09	1.11±0.23	1.13±0.26	1.22±0.22

Table III. Serum metabolites and lipid parameters quantified via 1H NMR spectroscopy. For each feature, the mean ⍰ standard deviation (std. error) is reported.

How to cite: Basoglu et al. NMR-based-Metabolomics Evaluation in Dogs Infected with Canine Parvovirus: A New Approach for Biomarker/s. Veterinaria Italiana, Vol. 61 No. 1 (2025) DOI: 10.12834/VetIt.3578.29616.2

	HC *vs* S ad. (*P*-value; Log_2FC)	HC *vs* S 72 h (*P*-value; Log_2FC)	HC *vs* NS (*P*-value; Log_2FC)	S ad. *vs* NS (*P*-value; Log_2FC)	S 72 h *vs* NS (*P*-value; Log_2FC)
Glucose	**0.01; -0.40**	**0.02; -0.27**	**0.02; -0.40**	0.76; -0.008	0.30; -0.13
Mannose	0.56; -0.09	0.47; -0.09	0.74; 0.09	0.36; 0.18	0.31; 0.18
Tyrosine	**0.001; 0.29**	**0.01; 0.16**	0.09; 0.17	0.47; -0.12	0.59; 0.01
Phenylalanine	**0.006; 0.31**	**0.04; 0.34**	0.07; 0.34	0.70; 0.03	0.59; 0.008
Cholate	0.20; 1.14	**0.04; 1.92**	0.75; 0.86	0.37; -0.28	0.08; -1.07
2-hydroxybutyrate	0.84; 0.31	0.74; 1.06	0.90; -0.27	0.62; -0.58	0.58; -1.34
Isovalerate	0.14; 0.52	0.05; 0.54	**0.004; 0.99**	0.05; 0.47	**0.03; 0.45**
Leucine	0.93; 0.18	0.58; 0.68	0.90; 0.54	0.96; 0.36	0.62; -0.13
Isoleucine	**0.002; 1.42**	**0.006; 1.37**	0.15; 0.83	**0.04; -0.59**	0.17; -0.54
Valine	0.10; 0.67	0.65; 0.53	0.27; 0.83	0.42; 0.17	0.70; 0.30
3-hydroxybutyrate	0.61; 0.34	0.87; 0.51	0.28; 0.19	0.36: -0.16	0.06; -0.32
Acetate	0.13; -0.22	0.07; 0.27	0.60; -0.09	0.16: 0.13	0.15; -0.36
Glutamate	0.11; -0.78	0.62; -0.26	**0.04; -1.30**	0.20: -052	**0.03; -1.04**
Pyroglutamate	0.67; -0.19	0.61; -0.16	0.31; -0.26	0.26: -0.06	0.42; -0.09
Citrate	**0.0006; -0.48**	**0.01; -0.97**	**0.002; -1.49**	0.78: -0.01	**0.03; -0.52**
Creatine	0.07; 0.41	0.79; 0.04	0.06; 1.03	0.14; 0.62	**0.01; 1.00**
Creatinine	**0.04; -0.60**	0.16; -0.36	0.65; -0.04	0.21; 0.55	0.38; 0.31
Dimethylsulfone	0.09; 0.88	0.31; 0.61	0.25; 0.84	0.56; -0.04	0.79; 0.23
Choline	0.91;0.003	0.82; 0.10	0.31; 0.28	0.12; 0.28	0.39; 0.18
Carnitine	**0.009;-0.62**	0.09; -0.37	**0.01; -0.59**	0.88; 0.03	0.36; -0.22
Betaine + TMAO	0.96; -0.09	0.72; -0.29	0.56; -0.26	0.28; -0.17	0.82; 0.03
Glycine	**0.002; -0.51**	0.012; -0.48	**0.01; -0.48**	0.70; 0.02	0.74; 0.0002
Glycerate	**0.002; -0.51**	**0.005; -0.38**	**0.008; -0.55**	0.74; -0.04	0.32; -0.17
Glycolate	0.06; 0.68	0.41; 0.37	**0.04; 1.46**	0.16; 0.78	**0.04; 1.09**
Fructose	**0.02; -0.29**	**0.03; -0.22**	**0.003; -0.30**	0.12; -0.09	0.18; -0.08
Lactate	**0.03; -0.29**	**3.29E-05; -0.49**	0.10; -0.26	0.88; 0.03	0.11; 0.23
Formate	**0.003; -0.37**	0.29; -0.13	**0.04; -0.39**	0.30; -0.02	0.05; -0.27
Alanine	0.61; 0.18	0.64; 0.11	0.29; 0.78	0.44; 0.60	0.10; 0.67

HC: healthy control, NS: non-survivors, S ad.: survivors at admission, S 72 h: survivors at hour 72.

Table IV. Univariate analysis was conducted to examine metabolites' variations among the four groups. Statistically significant P-values (P < .05) are indicated in bold.

Lipid-soluble extracts

RF classification algorithm was applied to investigate whether the different four groups (HC, S ad., S 72 h, NS) could be discriminated from the entire metabolic profiles. The results of the RF classification for each pairwise comparison are given in Figure 2, respectively. Overall, we obtained extremely robust classification models to discriminate between the different groups: HC *vs* S ad. (Accuracy = 87.5%), HC *vs* S 72 h (Accuracy = 100%), HC *vs* NS (Accuracy = 100%), S ad. *vs* NS (Accuracy = 88.4%), S 72 h *vs* NS (Accuracy = 86.1%), and S ad. *vs* S 72 h (Accuracy = 90%).

A total of 17 lipids were quantified in all ^{1}H NOESY spectra of lipid-soluble extracts, as shown in Table III. Univariate analysis was conducted to assess the variations in metabolites among the four groups (HC, S ad., S 72 h, NS), as presented in Table V. As observed in water-soluble extracts, the HC group exhibited the most distinct metabolic profile. Free cholesterol was higher in the other 3 groups compared with HC dogs. Esterified cholesterol was lower in S 72 h dogs compared with HC dogs. Fatty acyl chain CH_2CO, sphingomyelin, and glycerol backbone C-1, H2 C-3 H3 were higher in S 72 h and NS dogs compared with HC dogs, and also in NS dogs compared with S ad. dogs.

How to cite: Basoglu et al. NMR-based-Metabolomics Evaluation in Dogs Infected with Canine Parvovirus: A New Approach for Biomarker/s. Veterinaria Italiana, Vol. 61 No. 1 (2025) DOI: 10.12834/VetIt.3578.29616.2

	HC *vs* S ad.	HC *vs* S 72 h	HC *vs* NS	S ad. *vs* NS	S 72 h *vs* NS
	(*P*-value; Log_2FC)	(*P*-value; Log_2FC)	(*P*-value; Log_2FC)	(*P*-value; Log_2FC)	(*P*-value; Log_2FC)
Total cholesterol C-18 H3	0.07; -0.18	0.15; -0.16	0.21; 0.05	**0.007; 0.23**	**0.02; 0.22**
Fatty acyl chain $(CH_2)n$	0.35; -0.05	0.05; -0.09	0.23; -0.06	0.50-0.01;	0.76; 0.03
Total_cholesterol	0.06; -0.26	0.38; -0.12	0.07; -0.39	0.32;-0.14	0.12; -0.27
Fatty acyl chain $-CH_2CH$	0.19; -0.12	0.21; -0.10	0.83; -0.007	0.12; 0.11	0.09; 0.10
Fatty acyl chain $-CH_2CO$	0.35; 0.13	**0.03; 0.36**	**0.001; 0.59**	**0.0007; 0.47**	**0.03; 0.24**
Fatty acyl chain $CHCH_2CH$	**0.04; 0.15**	0.21; 0.06	0.31; 0.09	0.57; -0.05	0.66; 0.04
Phospolipids $n(CH_3)_3$	0.38; -0.05	**0.002; -0.14**	**0.006; -0.15**	0.05; -0.10	0.74; -0.01
Free_cholesterol_X	**0.04; 0.25**	**0.0001; 0.48**	**0.003; 0.41**	0.12; 0.16	0.42; -0.07
Glycerol backbone C-1 H2 C-3 H2	0.10; 0.49	**0.0002; 0.77**	**0.0003; 1.03**	**0.02; 0.53**	0.12; 0.26
Esterified cholesterol C-3 H	**0.0009; -0.35**	**0.02; -0.25**	0.19; -0.13	0.14; 0.22	0.23; 0.13
Phospoglicerides	0.84; -0.002	0.18; -0.07	0.13; -0.11	**0.005; -0.11**	0.47; -0.04
Fatty acyl chain -HC=CH-	0.29; 0.05	0.75: -0.002	0.21; 0.05	0.80; 0.006	0.24; 0.05
Sphingomyelin_CH=CH	0.33; 0.18	**0.0002; 0.43**	**0.001; 0.37**	**0.01; 0.20**	0.40; -0.05
Free cholesterol C-3 H	0.21; 0.50	0.15; 0.85	0.23; 0.61	0.67; 0.11	0.96; -0.24
Total cholesterol C-26 H3 C-27 H3	0.13; -0.18	0.27; -0.13	0.31; 0.06	**0.02; 0.23**	0.06; -0.07
Fatty acyl chain CH_3 $(CH_2)n$	0.99; 0.01	0.23; 0.04	0.83; -0.03	0.82; -0.04	0.26; 1.1
Esterified cholesterol C-19 H3	**0.001; -0.28**	**0.03; -0.25**	0.21; -0.15	0.28; 0.14	0.46; 0.42

HC: healthy control, NS: non-survivors, S ad.: survivors at admission, S 72 h: survivors at hour 72.

Table V. Univariate analysis was conducted to examine lipid variations among the four groups. Statistically significant P-values (P < .05) are indicated in bold.

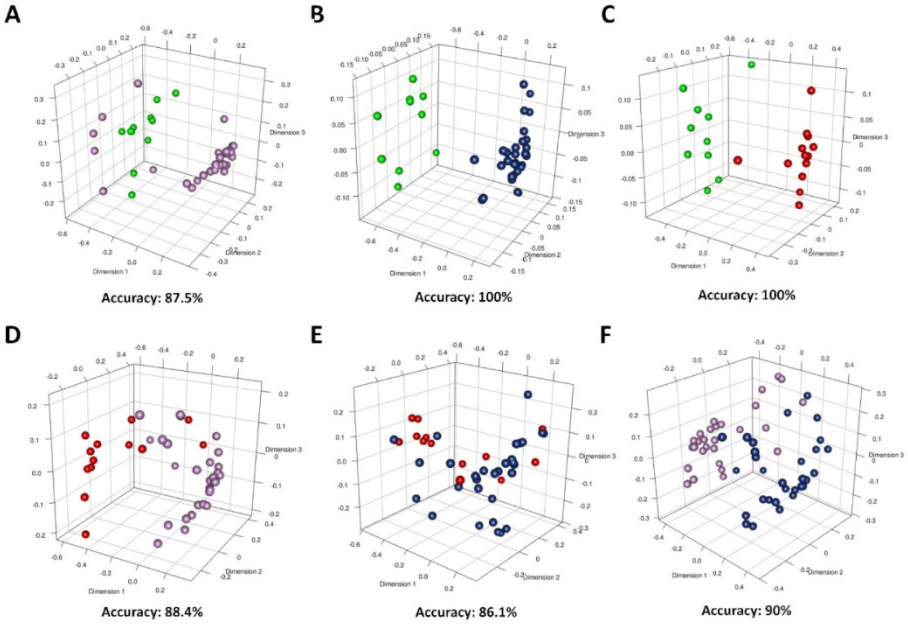

Figure 2. Random Forest (RF) model score plots. Each dot represents a single lipid-soluble serum lipidic profile colored by the different groups: A) HC (green dots) vs S ad. (violet dots) groups; B) HC (green dots) vs S 72 h (blue dots) groups; C) HC (green dots) vs NS (red dots) groups; D) S ad. (violet dots) vs NS (red dots) groups; E) S 72 h (blue dots) vs NS (red dots) groups; F) S ad. (violet dots) vs S 72 h (blue dots) groups. For each RF model performed the discrimination accuracy was also reported.

Discussion

NMR-based metabolomics was for the first time evaluated in CPV-infected dogs. Clinic signs and score, and cardiac troponin level were under the cited references (Ince et al., 2021; Oikonomidis et al., 2023). As a functional model, metabolomics can predict clinical aspects of microbe-host interactions (Bueno 2022). Progress has been made in understanding the role of inflammation, inflammatory metabolites, and lipids in infectious diseases (Tounta et al., 2021). Metabolomics has great potential to facilitate biomarker discovery in the study of idiopathic animal diseases and to improve our understanding of disease pathogenesis (Tran et al., 2020, Vignoli et al., 2023). In this study, S ad., S 72 h, and NS dogs had lower levels of glucose, fructose, and glyceric acid compared with HC dogs. The tricarboxylic acid (TCA) cycle has a key role in ATP production as well as in the synthesis of the biomolecules needed

How to cite: Basoglu et al. NMR-based-Metabolomics Evaluation in Dogs Infected with Canine Parvovirus: A New Approach for Biomarker/s. Veterinaria Italiana, Vol. 61 No. 1 (2025) DOI: 10.12834/VetIt.3578.29616.2

for viral replication Sanchez-Garcia et al., 2021) which is dependent on glucose, glutamine, and TCA cycles (Mayer et al., 2019). Infection can cause disease in the host, and metabolic intermediates of the TCA cycle, particularly citrate and succinate, are involved in this process (Schoeman et al., 2013). Citrate links also carbohydrate and fatty acid metabolism (Williams and O'Neill 2018). Fatty acid synthesis is important for the virus life cycle as it facilitates its entry, gene expression and replication, assembly, and release from the infected cells (Chukkapalli et al., 2012). In the present study, citrate was the most striking metabolite detected in water-soluble serum extract. It has a lower concentration level in S ad., S 72 h, and NS dogs compared with HC dogs. Because of the treatment, citrate level in 72 h dogs was increased significantly ($p < 0.004$) compared to S ad. dogs, it can be considered an important biomarker for recovery.

In animals, isoleucine plays an important role in the immune system, including the growth regulation of neutrophils and lymphocytes, the expression of host defense peptides that can regulate host innate and adaptive immunity, and the release of antibodies (Rivas-Santiago et al., 2011; Gu et al., 2019). Dietary L-isoleucine can improve growth and immunity; this may be derived from the fact that L-isoleucine treatment heals the body and modifies the immune system to activate the Pattern Recognition Receptors (PRRs) signaling pathway in porcine rotavirus (Mao et al., 2018). In the present study, isoleucine tends to have higher levels in S ad. and S 72 h dogs compared with HC dogs, and also in NS dogs than in S ad. dogs.

Formate is a toxic molecule that we believe may play a role in some diseases associated with single-carbon metabolism disorders (Lamarre et al., 2013). In the current condition, carnitine was found to be low in S ad. and NS dogs compared with HC dogs.

Alterations in phenylalanine metabolism are associated with sepsis caused by acute kidney injury. The main changes of the multi-omic network in sepsis are inflammatory response, platelet degranulation, myeloid activation in the immune system, phenylalanine, tyrosine and tryptophan biosynthesis, and arginine biosynthesis. In addition, some fatty acids with energy metabolism, such as 3-hydroxybutyrylcarnitine and L-hexanoylcarnitine, play an important role in lipid signal transduction (Chen et al., 2022). In this study, phenylalanine and tyrosine levels increased in S ad. and S 72 h dogs. These were also higher in NS dogs, although there was no statistical difference.

Carnitine is an important nutrient that aids in energy production and metabolism of fatty acids. Carnitine deficiency can cause endocrine diseases, cardiomyopathy, diabetes mellitus, malnutrition, aging, stomach pain, liver cirrhosis, etc., due to the abnormal regulation of carnitine. Clinicians may consider the use of thiamine in all sepsis patients at risk of thiamine deficiency, and the use of L-carnitine and vitamin C in patients with septic shock (Belsky et al., 2018; Alhasaniah 2023). Carnitine is an important essential nutrient that aids in energy production and fatty acid metabolism. In this study, carnitine was found to be low in S ad. and NS dogs.

The inhibitory neurotransmitter function of glycine is particularly important in the retina, brain, and spinal cord. In this role, it works by activating ionotropic glycine receptors, facilitating the entry of chloride ions, thereby hyperpolarizing neuronal membranes (Rusakov 2018). Evidence suggests that glycine is a gerontological agent capable of prolonging life and improving health in simple and complex diseases (Johnson and Cuellar 2023). In the present study, glycine was found to be low in S ad. and NS dogs.

Neuronal damage during infectious encephalomyelitis may result directly from the infectious agent or indirectly from the host's immune system. Excessive release of excitatory amino acid neurotransmitters such as glutamate may also contribute to neuronal death in neurodegenerative diseases and stroke. Neuroadaptive Sindbis virus activates neurotoxic pathways leading to abnormal glutamate receptor stimulation and neuronal damage (Nargi-Aizenman et al., 2004). Previous studies have reported that neutrophils express glutamate receptors and these cells can release glutamate, but the evidence for direct neutrophil-to-neutrophil communication has been elusive (Kopachet al., 2023). In the present study, glutamate was found to be low in NS dogs compared with HC and S 72 h dogs.

Using the entire water-soluble spectral information above, robust classification models to discriminate between the different groups were obtained suggesting that the infection significantly affects the canine metabolome. Surprisingly, there was relatively less differentiation observed between S ad. and NS dogs. This could be because probably in S 72 h dogs the animals start to revert to a healthy phenotype, also confirmed by the multivariate analysis (Table III). We observed that based on accuracy (91.3%) from multivariate analysis and Random Forest model score plots glucose, fructose, isovalerate, glutamate, citrate, carnitine, glycine, glycerate, and formate could be considered the most relevant biomarkers in CPV infection of dogs.

Phospholipids are important components of biological systems. The fatty acyl chain composition of phospholipids determines the biophysical properties of membranes and influences their effects on biological processes (Wang and Tontonoz 2019). Glycerophospholipids are phosphoglycerides that make up most of the lipid barrier of cell membranes (Opgenorth et al., 2020). Physiological free cholesterol/phospholipid ratios in cell membranes are necessary to maintain membrane fluidity (Jacobo-Albavera et al., 2021). As many inhibitors of sphingolipid

How to cite: Basoglu et al. NMR-based-Metabolomics Evaluation in Dogs Infected with Canine Parvovirus: A New Approach for Biomarker/s. Veterinaria Italiana, Vol. 61 No. 1 (2025) DOI: 10.12834/VetIt.3578.29616.2

metabolism are already in clinical use against other diseases, repurposing studies for applications in some viral infections appears to be a promising approach (Avota et al., 2021). Non-targeted lipidomic analysis shows that different types of sphingomyelins, lysophosphatidylcholine molecules, and lipophosphoserine molecules differ in dogs with sepsis (Montague et al., 2022). Sphingomyelin and acid sphingomyelinase can reduce infections by several viruses (*i.e.* adenovirus, Ebola virus, rhinovirus, and parvovirus) (Apple et al., 2008; Pakkanen et al., 2008; Pastenkos et al., 2019). In this study, the level of sphingomyelin was found to be higher in S 72 h and NS dogs compared to HC dogs, and also higher in NS dogs than in S ad. dogs. In addition, fatty acyl chain CH_2CO, glycerol backbone C-1 H2 C-3 H3, and free cholesterol were also higher in S ad. and S 72 h and NS dogs. Phosphoglycerides and phospholipids $n(CH_3)_3$ were also decreased in NS dogs.

As reported for the water-soluble spectra, also for lipid-soluble ones have a statistically significant and robust discriminatory accuracy between the different groups. All this highlight again how the metabolome varies drastically in the different pathophysiological conditions of the dogs considered in the study. We observed that, based on the accuracy (100%) from multivariate analysis and Random Forest model score plots fatty acyl chain CH_2CO, phospholipids, free and esterified cholesterols, glycerol backbone C-1 H2 C-3 H2 and sphingomyelin could be considered the most relevant biomarkers in CPV infection of dogs.

Conclusion

In conclusion, the findings of the current study suggest that NMR-based metabolomics (metabolites and lipids correctly identified and quantified in water- and lipid-soluble serum extract spectra) at admission and 72 h of commencement of treatment in CPV-infected puppies could be used as prognostic indicators. Citrate and fatty acyl chain CH_2CO could be predictive and prognostic values in CPV infection. Nonetheless, the measurement of the above markers should be combined with clinical score data for establishing an appropriate clinical judgment.

Funding and Acknowledgments

This work was financially supported by the Scientific and Technological Research Council of Turkey (TUBITAK, Project No: 221O599). The authors acknowledge Instruct-ERIC, a Landmark ESFRI project, and specifically the CERM/CIRMMP Italy Infrastructure for the NMR access provision financially supported by the EC Contract iNEXT No 653706. This article has been produced from R.O.Bicici's master thesis.

References

Al-Sulaiti, H., Almaliti, J., Naman, C.B., Al Thani, A.A., Yassine, H.M. (2023). Metabolomics approaches for the diagnosis, treatment, and better disease management of viral infections. Metabolites, 13, 948. doi: 10.3390/metabo13080948.

Alhasaniah, A.H. (2023). L-carnitine: Nutrition, pathology, and health benefits. Saudi J Biol Sci, 30, 103555. doi: 10.1016/j.sjbs.2022.103555.
Ali J, Khan R, Ahmad N, Maqsood I. Random forests and decision trees. Int J Adv Comput Sci Appl, (IJCSI), 9, 272.

Alves, F., Prata, S., Nunes, T., Gomes, J., Aguiar, S., Aires da Silva, F., Tavares, L., Almeida, V., Gil S. (2020). Canine parvovirus: a predicting canine model for sepsis. BMC Vet Res, 16(1), 199. doi:0.1186/s12917-020-02417-0.

Amaratunga, D., Cabrera, J., Lee, Y.S. (2008). Enriched random forests. Bioinformatics 24, 2010-2014. doi: 10.1093/bioinformatics/btn356.
Apple, FS, Murakami, MM, Ler, R, Walker, D, York, M. Analytical characteristics of commercial cardiac troponin I and T immunoassays, in serum from rats, dogs, and monkeys with induced acute myocardial injury. Clin Chem 54, 1982-1989, 2008. doi: 10.1373/clinchem.2007.097568.

Avota, E., Bodem, J., Chithelen, J, Mandasari, P., Beyersdorf, N., Schneider-Schaulies, J. (2021). The manifold roles of sphingolipids in viral infections. Front Physiol, 12, 715527. doi: 10.3389/fphys.2021.715527.

Basoglu, A., Baspinar, N., Tenori, L., Vignoli, A., Gulersoy, E. (2017). Effects of boron supplementation on peripartum dairy cows' health. Biol Trace Elem Res, 179, 218-225. doi 10.1007/s12011-017-0971-9.

Basoglu, A., Sen, I., Meoni, G., Tenori, L., Naseri, A. (2018). NMR-based plasma metabolomics at set intervals in newborn dairy calves with severe sepsis. Mediat Inflamm, 2018. doi: 10.1155/2018/8016510.

Basoglu, A., Baspinar, N., Tenori, L., Licari, C., Gulersoy, E. (2020). Nuclear magnetic resonance (NMR)-based metabolome profile evaluation in dairy cows with and without displaced abomasum. Vet Quart, 40, 1-15. doi: 10.1080/01652176.2019.1707907.

Belsky, J.B., Wira, C.R., Jacob, V., Sather, J.E., Lee, P.J. (2018). A review of micronutrients in sepsis: the role of thiamine, l-carnitine, vitamin C, selenium and vitamin D. Nutr Res Rev, 31, 281-290. doi: 10.1017/S0954422418000124.

Breiman, L. (2001). Random forests. Mach Learn 45, 5-32. doi: 10.1023/A:1010933404324.

Bueno, J. (2022). in Encyclopedia of Infection and Immunity. Metabolomics of infectious diseases. 387-397. doi: 10.1016/B978-0-12-818731-9.00095-1.

Chen, Q., Liang, X., Wu, T.Z., Jiang, J., Jiang, Y., Zhang, S., Ruan, Y., Zhang, H., Zhang ,C., Chen, P.., Lv, Y., Xin, J., Shi, D., Chen, X., Li, J., Xu, Y. (2022). Integrative analysis of metabolomics and proteomics reveals amino acid metabolism disorder in sepsis. J Transl Med, 20, 123. doi: 10.1186/s12967-022-03320-y.

Chen, T.L., Cao, Y., Zhang, Y.N., Liu, J., Bao, Y., Wang, C., Jia, W., Zhao, A. (2013). Random Forest in clinical metabolomics for phenotypic discrimination and biomarker selection. Evid-Based Compl Alt, 2013. doi: 10.1155/2013/298183.

Chukkapalli, V., Heaton, N.S., Randall, G. (2012). Lipids at the interface of virus–host interactions. Curr Opin Microbiol, 15, 512-518. doi: 10.1016/j.mib.2012.05.013.

Eregowda, C.G., De, U.K., Singh, M., Prasad, H., Akhilesh, A., Sarma, K., Roychoudhury, P., Rajesh, J.B., Patra, M.K., Behera, S.K. (2020). Assessment of certain biomarkers for predicting survival in response to treatment in dogs naturally infected with canine parvovirus. Microb Pathog, 149, 104485. doi: 10.1016/j.micpath.2020.104485.

Gu, C., Mao, X., Chen, D., Yu, B., Yang, Q. (2019). Isoleucine plays an important role for maintaining immune function. Curr Protein Pept Sci, 20, 644-651. doi: 10.2174/1389203720666190305163135.

Ince, M.E., Turgut, K., Naseri, A. (2021). Echocardiographic assessment of left ventricular systolic and diastolic functions in dogs with severe sepsis and septic shock; longitudinal study. Animals, 11, 2011. doi: 10.3390/ani11072011.

Jacobo-Albavera, L., Dominguez-Perez, M., Medina-Leyte, D.J., González-Garrido, A., Villarreal-Molina, T. (2021). The role of the ATP-binding cassette a1 (abca1) in human disease. Int J Mol Sci, 22, 1593. doi: 10.3390/ijms22041593.

Johnson, A.A., Cuellar, T.L. (2023). Glycine and aging: Evidence and mechanisms. Ageing Res Rev, 87. doi: 10.1016/j.arr.2023.101922.

Kopach, O., Sylantyev, S., Bard, L., Michaluk, P., Heller, J.P., Gutierrez Del Arroy, A., Ackland, G.L., Gourine, A.V., Rusakov, D.A. (2023). Human neutrophils communicate remotely via calcium-dependent glutamate-induced glutamate release. iScience, 26, 107236. doi: 10.1016/j.isci.2023.107236.

Lamarre, S.G., Morrow, G., Macmillan, L., Brosnan, M.E., Brosnan, J.T. (2013). Formate: an essential metabolite, a biomarker, or more? Clin Chem Lab Med, 51, 571-578. doi: 10.1515/cclm-2012-0552.

Ling, M., Norris, J.M., Kelman, M., Ward, M.P. (2012). Risk factors for death from canine parvoviral-related disease in Australia. Vet Microbiol, 158(3-4), 280-90. doi: 10.1016/j.vetmic.2012.02.034.

Mao, X., Gu, C., Ren, M., Chen, D., Yu, B., He, J., Yu, J., Zheng, P., Luo, J., Luo, Y., Wang, J., Tian, G., Yang, Q. (2018). l-isoleucine administration alleviates rotavirus infection and immune response in the weaned piglet model. Front Immunol, 9, 1654. doi: 10.3389/fimmu.2018.01654.

Mayer, K.A., Stöckl, J., Zlabinger, G.J., Gualdoni, G.A. (2019). Hijacking the supplies: metabolism as a novel facet of virus-host interaction. Front Immunol, 10, 1533. doi: 10.3389/fimmu.2019.01533.

Mazzaferro, E.M. (2020). Update on canine parvoviral enteritis. Vet Clin N Am-Small, 50, 1307-1325. doi: 10.1016/j.cvsm.2020.07.008.

Montague, B., Summers, A., Bhawal, R., Anderson, E.T., Kraus-Malett, S., Zhang, S., Goggs, R. (2022). Identifying potential biomarkers and therapeutic targets for dogs with sepsis using metabolomics and lipidomics analyses. Plos One, 17, e0271137. doi: 10.1371/journal.pone.0271137.

Mylonakis, M.E., Kalli, I., Rallis, T.S. (2016). Canine parvoviral enteritis: an update on the clinical diagnosis, treatment, and prevention. Vet Med-Res Rep, 7, 91-100. doi: 10.2147/VMRR.S80971.

Neuhäuser, M. (2011). Wilcoxon–Mann–Whitney Test. In: Lovric M, ed. International Encyclopedia of Statistical Science. Berlin, Heidelberg: Springer Berlin Heidelberg, 1656-1658. doi: 10.1007/978-3-642-04898-2_615.

Nargi-Aizenman, J.L., Havert, M.B, Zhang, M., Irani, D.N., Rothstein, J.D., Griffin, D.E. (2004). Glutamate receptor antagonists protect from virus-induced neural degeneration. Ann Neurol, 55, 541-549. doi: 10.1002/ana.20033.

Navarro, C., Cáceres, A., Gaggero, A. (2020). Detection of canine parvovirus in dogs using polymerase chain reaction. Am J Biomed Sci and Res, 7(6), 540-547. doi: 10.34297/AJBSR.2020.07.001219.

Nguyen, S.V., Umeda, K., Yokoyama, H., Tohya, Y., Kodama, Y. (206). Passive protection of dogs against clinical disease due to Canine parvovirus-2 by specific antibody from chicken egg yolk. Can J Vet Res, 70, 62-64.

Oikonomidis, I.L., Theodorou, K., Papaioannou, E., Xenoulis, P.G., Adamama-Moraitou, K.K., Steiner, J.M., Kritsepi-Konstantinou, M., Suchodolski, J.S., Rallis, T., Soubasis, N. (2023). Serial measurement of cardiac troponin I in hospitalized dogs with canine parvoviral enteritis: Association with outcome and canine pancreas-specific lipase concentration. Res Vet Sci, 157, 1-5. doi: 10.1016/j.rvsc.2023.02.004.

Opgenorth, J., Sordillo, LM, Lock, A.L., Gandy., J.C., VandeHaar, M.J. (2020). Colostrum supplementation with n-3 fatty acids alters plasma polyunsaturated fatty acids and inflammatory mediators in newborn calves. J Dairy Sci, 103, 11676-11688. doi: 10.3168/jds.2019-18045.

Pacheco-Navarro, A.E., Rogers, A.J. (2023). The Metabolomics of critical illness. Handb Exp Pharmacol, 277, 367-384. doi: 10.1007/164_2022_622.

Pakkanen, K., Karttunen, J., Virtanen, S., Vuento, M. (2008). Sphingomyelin induces structural alteration in canine parvovirus capsid. Virus Res, 132, 187-191. doi: 10.1016/j.virusres.2007.10.008.

Pastenkos, G., Miller, J.L., Pritchard, S.M., Nicola, A.V. (2019). Role of sphingomyelin in alphaherpesvirus entry. Virol J, 93, e01547-18. doi: 10.1128/JVI.01547-18.

Rusakov, D.A. (2018). An optical sensor to monitor the dynamics of extracellular glycine. Nat Chem Biol, 14, 835-836. doi: 10.1038/s41589-018-0123-3.

Rivas-Santiago, C.E., Rivas-Santiago, B., Leon, D.A., Castañeda-Delgado, J., Hernández Pando, R. (2011). Induction of beta-defensins by l-isoleucine as novel immunotherapy in experimental murine tuberculosis. Clin Exp Immunol, 164, 80-89. doi: 10.1111/j.1365-2249.2010.04313.x.

Sanchez-Garcia, F.J., Perez-Hernandez, C.A., Rodriguez-Murillo, M., Moreno-Altamirano, M.M.B. (2021). The role of tricarboxylic acid cycle metabolites in viral infections. Front Cell Infect Mi, 14, 11, 72504311. doi: 10.3389/fcimb.2021.725043.

Schoeman, J.P., Goddard, A., Leisewitz, A.L. (2013). Biomarkers in canine parvovirus enteritis. New Zeal Vet J, 61, 217-222. doi: 10.1080/00480169.2013.776451.

Sullivan, L.A. (2019). Parvoviral Enteritis: What's New? Adv Small Anim Med Surg, 32, 1–3. doi: 10.1016/j.asams.2019.11.001.

Tounta, V., Liu, Y., Cheyne, A., Larrouy-Maumus, G. (2021). Metabolomics in infectious diseases and drug discovery. Mol Omics, 17, 376-393. doi: 10.1039/d1mo00017a.

Tran, H., McConville, M., Loukopoulos, P. (2020). Metabolomics in the study of spontaneous animal diseases. J Vet Diagn Invest, 32, 635-647. doi: 10.1177/1040638720948505.

Vignoli, A., Meoni, G., Ghini, V., Di Cesare, F., Tenori, L., Luchinat, C., Turano, P. (2023). NMR-based metabolomics to evaluate individual response to treatments. Handb Exp Pharmacol, 277, 209-245. doi: 10.1007/164_2022_618.

Vignoli, A., Ghini, V., Meoni, G., Licari, C., Takis, P.G., Tenori, L., Turano, P., Luchinat, C. (2019). High-throughput metabolomics by 1D NMR. Angew Chem Int Ed Engl, 58, 968-994. doi: 10.1002/anie.201804736.

Wang, B., Tontonoz, P. (2019). Phospholipid remodeling in physiology and disease. Annu Rev Physiol, 81, 165-188. doi: 10.1146/annurev-physiol-020518-114444.

Wilcoxon, F. (1945). Individual Comparisons by Ranking Methods. Biometrics Bulletin 1, 80-83.

Williams, N.C., O'Neill, L.A.J. (2018). A Role for the Krebs Cycle Intermediate citrate in metabolic reprogramming in innate immunity and inflammation. Front Immunol, 9, 141. doi: 10.3389/fimmu.2018.00141.